Dalton Transactions

Accepted Manuscript

ROYAL SOCIETY OF CHEMISTRY

www.rsc.org/dalton

$Na_2Co_2Fe(PO_4)_3$ crystallizes with the alluaudite-type structure (S.G. *C*2/*c*) and plays a dual anode/cathode behavior in sodium ion battery.

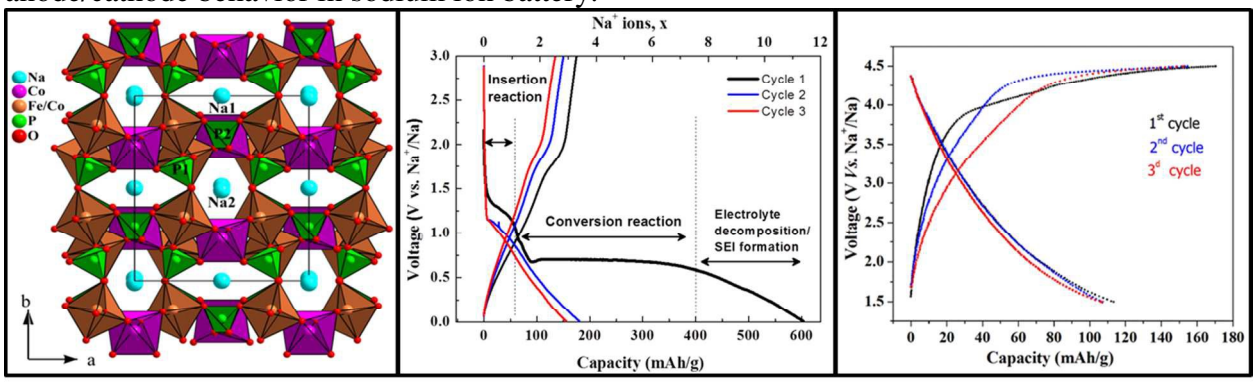

Dalton Transactions

RSCPublishing

ARTICLE

Alluaudite $Na_2Co_2Fe(PO_4)_3$ as electroactive material for sodium ion batteries

Cite this: DOI: 10.1039/xoxxoooooox

R. Essehli,[a,*] I. Belharouak,[a,*] H. Ben Yahia,[a,*] K. Maher,[a] A. Abouimrane,[a] B. Orayech,[b] S. Calder,[c] X. L. Zhou,[d] Z. Zhou,[d] and Y-K. Sun.[e]

Received ooth January 2012,
Accepted ooth January 2012

DOI: 10.1039/xoxxoooooox

www.rsc.org/

The electroactive orthophosphate $Na_2Co_2Fe(PO_4)_3$ was synthesized using a solid state reaction. Its crystal structure was solved using the combination of powder X-ray- and neutron-diffraction data. This material crystallizes according to the alluaudite structure (S.G. *C*2/*c*). The structure consists of edge sharing [MO_6] octahedra (*M*= Fe, Co) resulting in chains parallel to [-101]. These chains are linked together via the [PO_4] tetrahedra to form two distinct tunnels in which sodium cations are located. The electrochemical properties of $Na_2Co_2Fe(PO_4)_3$ were evaluated by galvanostatic charge-discharge cycling. During the first discharge to 0.03V, $Na_2Co_2Fe(PO_4)_3$ delivers a specific capacity of 604 mAh/g. This capacity is equivalent to the reaction of more than seven sodium ions per formula unit. Hence, this is a strong indication of a conversion-type reaction with the formation of metallic Fe and Co. The subsequent charge and discharge involved the reaction of fewer Na ions as expected for a conversion reaction. When discharged to 0.9 V, the material intercalated only one Na^+-ion leading to the formation of the new phase $Na_3Co_2Fe(PO_4)_3$. This phase could then be cycled reversibly with an average voltage of 3.6 V *vs.* Na^+/Na and a capacity of 110 mAh/g. This result is in good agreement with the theoretical capacity expected from the extraction/insertion of two sodium atoms in $Na_3Co_2Fe(PO_4)_3$.

1. Introduction

Due to their environmental compatibility and low cost, iron-based phosphate compounds have been intensively explored as electroactive materials during the last decade. Moreover, their reasonable energy density, enhanced safety and of the diversity of their structural frameworks make them of interest as positive or negative electrode materials for both lithium and sodium ion batteries.[1,6] Of significance, one can cite phosphates whose crystal structures comprise cavities and tunnels such as $FePO_4$, $NaFePO_4$, $[Na_{1-x}Li_x]MnFe_2(PO_4)_3$, $Na_2Fe_{3-x}Mn_x(PO_4)_3$, $Na_3Fe_3(PO_4)_4$, $Na_2Fe(P_2O_7)$, $Na_4Fe_3(PO_4)_2(P_2O_7)$, $Na_3Fe(PO_4)(CO_3)$ and Na_2FePO_4F.[7-15]

Our group recently reported on the preparation and electrochemical performance of a new orthophosphate α-$Na_2Ni_2Fe(PO_4)_3$.[16] The electrochemical results for this new phase, tested as anode material, indicated that during the first discharge to 0.03 V *vs.* Na^+/Na, the material delivers a capacity of 960 mAh/g. This capacity corresponds to the reaction of more than seven sodium atoms per formula unit, which indicates a conversion-type behavior with the formation of metallic Fe and Ni. In addition, we demonstrated that this kind of materials has the ability to be used as a cathode material. Indeed, $Na_2Ni_2Fe(PO_4)_3$ can insert one Na^+ ion which leads to the formation of $Na_3Ni_2Fe(PO_4)_3$.[16] This compound can be hence charged and delivers a capacity of 160 mAh/g at 3.6V *vs.* Na^+/Na. It is worth nothing that $LiFePO_4$, which is one of the mainstream cathodes in the Li-ion battery technology, can deliver a capacity of 160 mAh/g at 3.45V *vs.* Li^+/Li.[17,18]

In order to search for new sodium based compounds, we herein report on the synthesis, crystal structure determination, and the electrochemical properties of the orthophosphate $Na_2Co_2Fe(PO_4)_3$. This material and its sodiated homologous $Na_3Co_2Fe(PO_4)_3$ are studied as anode and cathode materials for sodium ion batteries, respectively.

2. Experimental Section

2.1. Synthesis

In typical solid state reaction, a stoichiometric mixtures of Na_2CO_3 (Aldrich, 99.5 %), $Co(NO_3)_2$•$6H_2O$ (Merck, 99.9 %), $Fe(NO_3)_3$•$9H_2O$ (Merck, 99 %), and $NH_4H_2PO_4$ (Aldrich, 99.99 %) were ground in an agate mortar, then the powder mixture was transferred into a platinum crucible and heated at 200°C for 6 h and at 500 °C for 24 h in air in order to release H_2O, NH_3, and CO_2. The obtained powder was then ground and calcined at 850 °C for 48 h.

2.2. Powder X-Ray diffraction measurements

The sample was characterized by high precision powder X-ray diffraction (PXRD), using a Panalytical diffractometer operating with Cu*K*α radiations. The sample was scanned between 10 and 120 (°). Full pattern matching refinement was performed with the Jana2006 program package.[19] The background was estimated by a Legendre function, and the peak shapes were described by a pseudo-Voigt function. The refinement of peak asymmetry was performed using four Berar-Baldinozzi parameters (Fig. S1). Evaluation of these data

revealed the refined cell parameters a = 11.7522 Å, b = 12.4489 Å, c = 6.4534 Å, β = 114.06 (°), and V = 862.12 Å^3.

2.3. Neutron powder diffraction

Neutron powder diffraction (NPD) data were collected on the high-resolution diffractometer HB-2A at the High Flux Isotope Reactor of Oak Ridge National Laboratory, using neutrons of wavelength 2.413 Å. For the measurements, the sample in the form of ~3 g of powder was loaded in a vanadium can and the data were collected at 290 K using a top-loading closed-cycle refrigerator. The Rietveld analysis of the data was performed using the Fullprof Suite[20] and Jana2006 program packages.

Table 1. Crystallographic and structure refinements data for $Na_2Co_2Fe(PO_4)_3$

Rietveld Refinement	
Crystal data	
Chemical formula	$Na_2Co_{1.935}Fe_{1.065}P_3O_{12}$
M_r	504.4
Crystal system	Monoclinic
Space group	*C*2/*c*
Temperature (K)	290
a (Å)	11.7599 (3)
b (Å)	12.4522 (3)
c (Å)	6.44063 (16)
β (°)	113.913 (2)
V (Å^3)	862.18 (4)
Z	4
Data collection	
Diffractometer	HB-2A
Radiation type	λ = 2.413 Å
$2\theta_{min}$, $2\theta_{step}$, $2\theta_{max}$ values (°)	17.63, 0.05, 123.98
Refinement	
R_p	0.024
R_{wp}	0.030
R_{exp}	0.039
$R(F)$	0.011
R_{Bragg}	0.016
goodness of fit χ^2	0.578
No. of data points	2380
No. of parameters	59
Profile function	Pseudo-Voigt
Background	Chebyshev function with15 terms

2.4. Electrochemical cycling

The positive electrode was prepared by spreading a mixture of 80% $Na_2Co_2Fe(PO_4)_3$ powder (active material), 15% super-P (conductive additive) and 5% of polyvinylidene difluoride (PVDF binder) onto a copper foil, and drying at 100°C overnight. The electrolyte was made of 1 M $NaPF_6$ salt dissolved in ethylene carbonate (EC) and dimethyl carbonate (DMC) solvent combination. Metallic sodium was used as the negative electrode. Coin cells (CR2032) comprising [$Na_2Co_2Fe(PO_4)_3$/$NaPF_6$-EC-DMC/Na] were assembled inside an argon-filled glove box. Electrochemical performances were evaluated by galvanostatic charge-discharge cycling at 10 mA/g, in the voltage range of 0.03–3.0 V *vs.* Na^+/Na. The sodiated $Na_3Co_2Fe(PO_4)_3$ phase was obtained by discharging the pristine material electrode $Na_2Co_2Fe(PO_4)_3$ down to 0.9 V. The $Na_3Co_2Fe(PO_4)_3$ electrode was then washed several times with EC, dried, and used as a positive electrode. The $Na_3Co_2Fe(PO_4)_3$/$NaPF_6$-EC-DMC/Na coin-type cells were cycled using a constant current charge–discharge at a rate of 5 mA/g in the voltage range of 1.8–4.5 V *vs.* Na^+/Na.

3. RESULTS AND DISCUSSION

3.1. Structure refinement

The crystal structure of $Na_2Co_2Fe(PO_4)_3$ was solved using the crystal structure of $Na_2Fe_3(PO_4)_3$ as a starting structural model.[21] A Co/Fe statistical disorder has been introduced over the two crystallographic sites of iron [4*e* (0 0.272 1/4) and 8*f* (0.781 0.156 0.368)]. The refinement of the occupancies indicated the presence of iron mainly at the 8*f* atomic position, leading to the chemical composition $Na_2Co_{1.935}Fe_{1.065}P_3O_{12}$ which is in perfect agreement with the expected composition $Na_2Co_2Fe(PO_4)_3$. Since, few atomic displacement parameter (ADP) tensors displayed negative values; atoms of the same nature have been restricted to have the same ADPs. The Rietveld analysis of the neutron powder diffraction data collected at 290 K led to the reliability factors listed in Table. 1 [Rp = 2.3%, wRp = 2.9%, R_B = 1.4%]. The final atomic positions are given in Table. 2. Fig. 1 shows a good agreement between the experimental and calculated patterns.

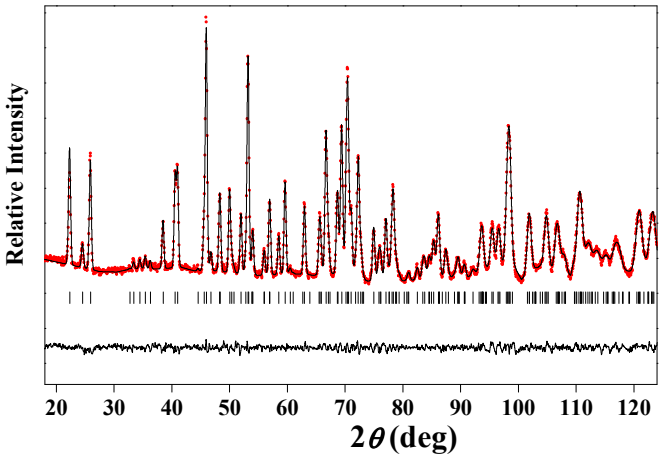

Fig. 1. Observed, calculated and difference plots for neutron powder diffraction of $Na_2Co_2Fe(PO_4)_3$ collected at 290 K.

3.2 Crystal Structure

$Na_2Co_2Fe(PO_4)_3$ is isostructural with $Na_2Fe_3(PO_4)_3$.[21] The structure consists of edge-sharing MO_6 (M= Co, Fe) octahedra running along the [-101] axis (Fig. 2b). The MO_4 infinite chains are cross connected by the PO_4 tetrahedra giving rise to channels along the [001] axis, within which eight-coordinated sodium atoms are located (Figs. 2a, 2c). The interatomic distances and bond valence sums (BVS) [22, 23] are listed in Table 3.

The d(Co1-O) distances range from 2.074 to 2.182 Å with an average distance of 2.142 Å which is in good agreement with the value of 2.145 Å calculated from the sum of the effective ionic radii of the six-coordinated high spin $Co1^{2+}$ and O^{2-}.[24] The d(Co2-O) distances range from 1.945 to 2.160 Å with an average distance of 2.048 Å. This would indicate that $Co2^{2+}$ is at the low spin state, since in this case the distance d(Co-O) was reported to be 2.05 Å.[25] Moreover, it should be noted that there is a statistical disorder between $Co2^{2+}$ and $Fe2^{3+}$ at the 8*f* atomic position (0.781 0.156 0.368). The BVS values of 1.795 and 2.331 indicate that Co1 is under bonded, whereas Co2 is over bonded.

Table 2. Atom positions and isotopic displacement parameters for $Na_2Co_2Fe(PO_4)_3$ from neutron diffraction data at 290 K.

Atom	Wyck.	Occ.	*x*	*y*	*z*	U_{iso} (Å^2)
Na1	4*b*	1	0	1/2	1/2	0.051(2)
Na2	4*e*	1	1/2	0.4872(8)	1/4	0.051(2)
Co1/Fe1	4*e*	0.993/0.007	0	0.2723(9)	1/4	0.031(7)
Co2/Fe2	8*f*	0.476/0.524	0.7816(3)	0.1566(2)	0.3682(6)	0.0030(18)
P1	8*f*	1	0.7646(3)	0.1101(3)	0.8780(7)	0.0127(14)
P2	4*e*	1	0	0.2936(5)	3/4	0.0127(14)
O1	8*f*	1	0.8383(3)	0.1670(2)	0.1086(6)	0.0145(9)
O2	8*f*	1	0.0412(3)	0.2197(3)	0.9668(7)	0.0145(9)
O3	8*f*	1	0.7778(3)	0.1778(2)	0.6852(5)	0.0145(9)
O4	8*f*	1	0.8252(2)	0.0011(4)	0.3868(5)	0.0145(9)
O5	8*f*	1	0.6028(3)	0.1343(2)	0.2511(5)	0.0145(9)
O6	8*f*	1	0.8740(3)	0.3981(3)	0.1734(6)	0.0145(9)

Table 3. Interatomic distances (in Å) and bond valences (B.V.) of $Na_2Co_2Fe(PO_4)_3$. Average distances are given in brackets.

	distance
Na1-O5	2.300
Na1-O6	2.388
Na1-O6	2.529
Na1-O5	2.898
	<2.529>
	[a] 1.318 [8]
Na2-O4	2.413
Na2-O4	2.550
Na2-O1	2.838
Na2-O2	2.877
	<2.669>
	[a] 0.882 [8]
Co1-O6	2.074
Co1-O2	2.169
Co1-O1	2.182
	<2.142>
	[a] 1.795 [6]
Co2/Fe2-O5	1.945
Co2/Fe2-O4	1.994
Co2/Fe2-O1	2.039
Co2/Fe2-O2	2.072
Co2/Fe2-O3	2.078
Co2/Fe2-O3	2.160
	<2.048>
	[a] 2.331/2.794[6]
P1-O6	1.529
P1-O4	1.548
P1-O1	1.554
P1-O3	1.559
	<1.548>
	[a] 4.83 [4]
P2-O5	1.503
P2-O2	1.576
	<1.539>
	[a] 4.96 [4]

[a] bond valence sum, B.V. = $e^{(r0-r)/b}$ with the following parameters: b = 0.37, r_0 (Na^I–O) = 1.803, r_0 (Co^{II}–O) = 1.692, r_0 (Fe^{III}–O) = 1.759, and r_0 (P^V–O) = 1.617 Å.[22, 23]

The $P1O_4$ tetrahedra are quite regular, however the $P2O_4$ tetrahedra are distorted. The distances range from 1.529 to 1.559 Å and from 1.503 to 1.576 Å with the average values of 1.548 Å and 1.539 Å for P1 and P2, respectively. These values are consistent with the value of 1.55 Å calculated from the sum of the effective ionic radii of the four-coordinated P^{5+} and O^{2-}.[24] The BVS values of 4.83 and 4.96 are in agreement with the expected value of +5 for P^{+5}, which is of the same order of magnitude reported for $Na_2Ni_2Fe(PO_4)_3$.[17]

The $Na1^+$ and $Na2^+$ cations are bonded to eight oxygen atoms (Fig. 2c). The Na1-O and Na2-O distances range from 2.300 to 2.898 Å and from 2.413 to 2.877 Å with the average values of 2.529 Å and 2.669 Å, respectively. The BVS values of 1.318 and 0.882 indicate that Na1 and Na2 are overbonded and underbonded, respectively. Even if the coordination sphere of Na1 is decreased to six, Na1 remains overbonded with a BVS value of 1.214.

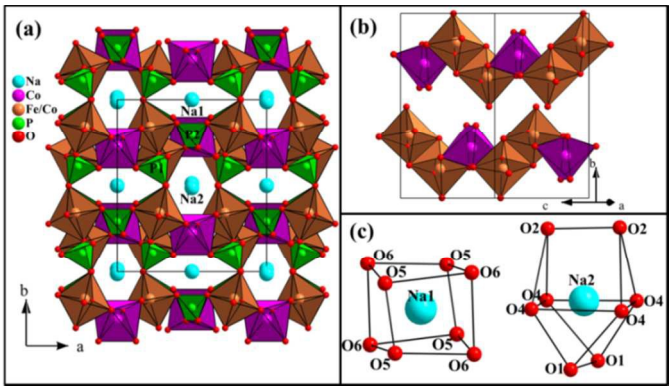

Fig. 2. (a) Projection view of $Na_2Co_2Fe(PO_4)_3$ along the [001] axis , (b) View of the edge-sharing octahedra running along [-101], and (c) Coordination spheres of the Na1 and Na2 cations.

3.3. Electrochemical properties

3.3.1. $Na_2Co_2Fe(PO_4)_3$ as an anode material for sodium batteries

The electrochemical performances of the studied electrodes were evaluated at room temperature. Fig. 3a shows the first three cycles of the [$Na_2Co_2Fe(PO_4)_3$/$NaPF_6$-EC-DMC/Na] cell cycled between 3 and 0.03 V at the 10 mA/g current density. The initial discharge capacity of 604 mAh/g is much higher than the theoretical capacity of 371.8 mAh/g arising from the consecutive reduction of Fe^{3+} to Fe^0 and 2 Co^{2+} to 2 Co^0. The additional 230 mAh/g capacity is most probably due to the reduction of the electrolyte over the positive electrode.[25-28] The first discharge can be segregated to three voltage regions (Fig. 3). The first region can be observed as a plateau upon the

discharge to around 0.9 V where the cell delivered a capacity of 65 mAh/g. This capacity is close enough to the insertion of a one sodium atom per formula unit owing to the reduction of Fe^{3+} to Fe^{2+}. Similar results were observed in other phosphate materials such as $NaMnFe_2(PO_4)_3$ and α-$Na_2Ni_2Fe(PO_4)_3$.[8,17] The second voltage region consists of a long plateau that ends at around 0.6 V, and the capacity (325 mAh/g) associated with it corresponds to the conversion reaction of Fe^{2+} and Co^{2+} to their metallic forms. Below 0.6 V, the observed voltage slope and the capacity associated with it are attributed to the reduction of the electrolyte and/or the formation of solid electrolyte interface (SEI).

The second and third discharge profiles are different from the 1st one because during the first discharge to 0V the $Na_2Co_2Fe(PO_4)_3$ structure collapsed in an irreversible process. In the first discharge, some of the obtained capacity is related to the electrolyte decomposition and the formation of the solid electrolyte interface (SEI). The same behavior has been observed in various oxyphosphates such as $M_{0.5}TiOPO_4$ (M= Ni, Co and Fe).[24-27]

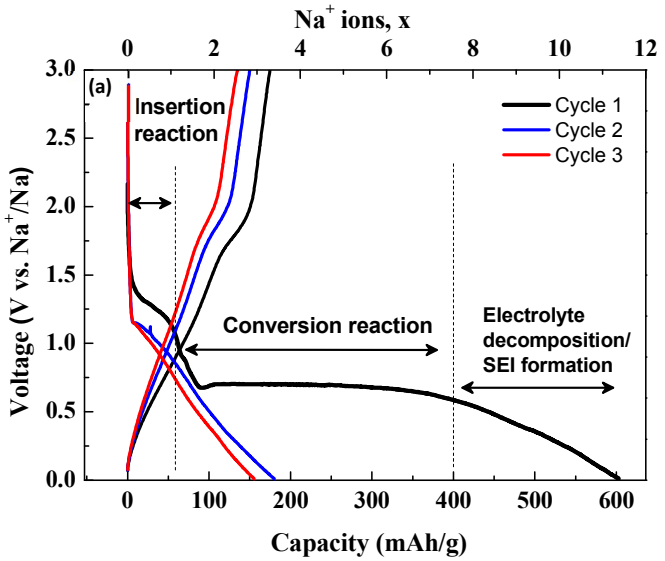

Fig. 3a. Charge-discharge curves of $Na/Na_2Co_2Fe(PO_4)_3$ cell between 3 and 0.03 V at the current density of 10 mA/g.

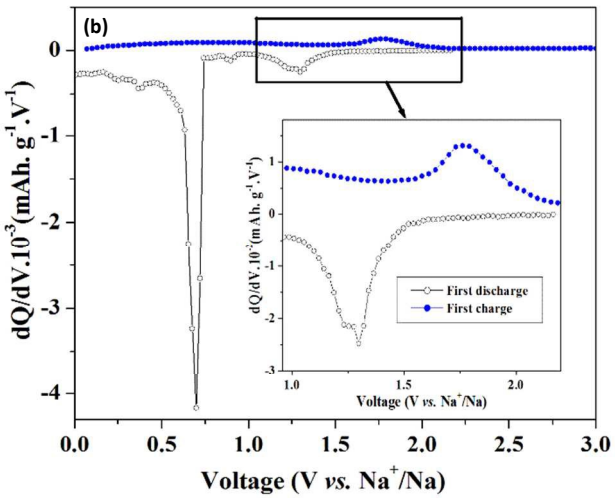

Fig. 3b. The differential galvanostatic profiles (dQ/dV) of $Na_2Co_2Fe(PO_4)_3$

Fig. 3b shows the differential galvanostatic profile (dQ/dV) of $Na_2Co_2Fe(PO_4)_3$ material. The first cycle profile shows three reduction peaks and one oxidation peak. For the first discharge scan the minor peak, at 1.30V, is assigned to iron reduction from Fe^{3+} to Fe^{2+}. The major peak centered at 0.63V has been attributed to the irreversible process by which the reduction of Fe^{2+} and Co^{2+} to their metallic forms occur. This phenomenon was reported for $FePO_4$[29], $LiFePO4$[30] and $M_{0.5}TiOPO_4$ (M= Ni, Co and Fe).[25-28] The third minor peak at 0.36V can be attributed to the decomposition of the electrolyte, which results in the formation of the solid electrolyte interphase (SEI) film. During the charge, one broad peak is observed around ~1.76 V and corresponds to the oxidation of metallic Fe and Co.[25,28-30]

3.3.2. $Na_2Co_2Fe(PO_4)_3$ as a cathode material for sodium batteries

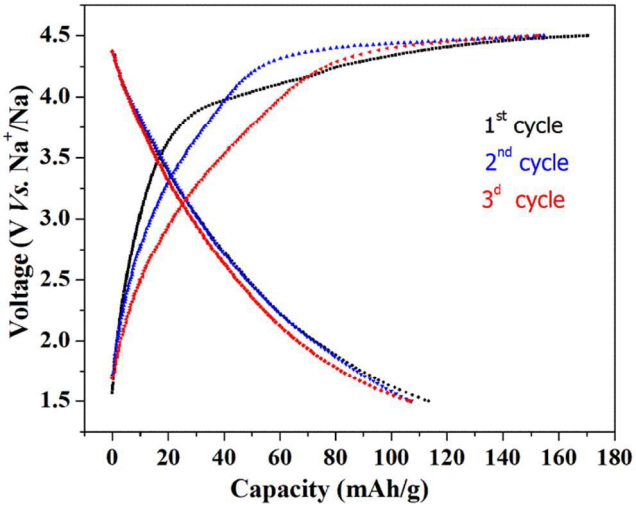

Fig. 4. Charge-discharge profiles of $Na/Na_3Co_2Fe(PO_4)_3$ cell between 1.5–4.5 V at the current rate 5 mA/g.

$Na_3Co_2Fe(PO_4)_3$ was obtained through the partial sodiation of $Na_2Co_2Fe(PO_4)_3$ upon discharge to 0.9 V and its PXRD is very similar to that of $Na_2Co_2Fe(PO_4)_3$ (Fig. S2). The electrochemically prepared material was then evaluated as a cathode by a galvanostatic charge-discharge cycling under the 5 mA/g current rate in the voltage range 1.5–4.5 V *vs.* Na^+/Na (Fig. 4). When charged to 4.5 V, $Na_3Co_2Fe(PO_4)_3$ displays a sloppy voltage profile *vs.* Na^+/Na with a first charge capacity of 170 mAh/g. This capacity is slightly higher than 152 mAh/g, corresponding to the removal of three sodium atoms. The electrolyte oxidation may have contributed to the excess of capacity. This capacity and voltage profile are similar to the ones reported for $Na_3Ni_2Fe(PO_4)_3$, $Na_2Fe_3(PO_4)_3$ and $NaFePO_4$.[5,14,17] By analogy to these works, the observed capacity of $Na_3Co_2Fe(PO_4)_3$ arises from the consecutive oxidation of Fe^{2+} to Fe^{3+} and 2 Co^{2+} into 2 Co^{3+}. Extensive investigations are needed to better understand the electrochemical reaction mechanism of the sodium storage in both $Na_2Co_2Fe(PO_4)_3$ and $Na_3Co_2Fe(PO_4)_3$.

4. Conclusion

The new orthophosphate $Na_2Co_2Fe(PO_4)_3$ was successfully synthesized by a solid state reaction route. PXRD and NPD confirmed the formation of a pure phase, which crystallizes with the alluaudite-type structure. When discharged to 0.03V *vs.* Na^+/Na, $Na_2Co_2Fe(PO_4)_3$ delivered a capacity of 604 mAh/g which is higher than the predicted theoretical capacity of 371.8

mAh/g. The large irreversible capacity observed during the first discharge can be mainly attributed to the conversion reaction and the formation of the SEI film and decomposition of the electrolyte. When the discharge is limited to 0.9 V *vs.* Na^+/Na, $Na_2Co_2Fe(PO_4)_3$ intercalates one sodium atom forming the sodiated phase $Na_3Co_2Fe(PO_4)_3$. The electrochemical tests proved the ability of this material to be useful as cathode material for sodium ion batteries.

Acknowledgement

Neutron diffraction was conducted at ORNL's High Flux Isotope Reactor sponsored by the Scientific User Facilities Division, Office of Basic Energy Sciences, U.S. Department of Energy.

Notes and references

[a] Qatar Environment and Energy Research Institute, Qatar Foundation, P.O. Box 5825, Doha, Qatar.
[b] Departamento de Física de la Materia Condensada, Universidad del País Vasco, P.O. Box 644, Bilbao, Spain.
[c] Quantum Condensed Matter Division, Oak Ridge National Laboratory, Oak Ridge, TN 37831, USA.
[d] Institute of New Energy Material Chemistry, Nankai University, Tianjin 300071, China.
[e] Department of Energy Engineering Hanyang University, 17 Haengdang-dong, Seongdong-gu, Seoul, 133-791, Korea

Corresponding authors:
H. Ben Yahia (Hyahia@qf.org.qa)
R. Essehli (ressehli@qf.org.qa)
I. Belharouak (ibelharouak@qf.org.qa)

† Electronic Supplementary Information (ESI) available: See DOI: 10.1039/b000000x/

1 N. Recham, J.-N. Chotard, L. Dupont, K. Djellab, M. Armand and J.M. Tarascon*, J. Electrochem. Soc.,* 2009, **156**, 993.
2 Y. Kawabe, N. Yabuuchi, M. Kajiyama, N. Fukuhara, T. Inamasu, R. Okuyama, I. Nakai and S. Komaba, *Electrochem. Commun*., 2011, **13**, 1225.
3 S. P. Ong, V. L. Chevrier, G. Hautier, A. Jain, C. Moore, S. Kim, X. Ma and G. Ceder, *Energ. Environ. Sci*., 2011, **4**, 3680.
4 M. Nose, H. Nakayama, K. Nobuhara, S. Nakanishi, and H. Iba, *J. Power Sources.*, 2013, **234**, 175.
5 M. Nose, S. Shiotani, H. Nakayama, K. Nobuhara, S. Nakanishi, and H. Iba, *Electrochem. Commun.*, 2013, **34**, 266.
6 Y. Dong, S. Li, K. Zhao, C. Han, W. Chen, B. Wang, L. Wang, B. Xu, Q. Wei, L. Zhang, X. Xu and L. Mai, *Energy Environ. Sci..*, 2015, **DOI: 10.1039/C5EE00036J**
7 K. Zaghib, J. Trottier, P. Hovington, F. Brochu, A. Guerfi, A. Mauger and J.M.C Julien, *Power Sources.,* 2011, **196**, 9612.
8 P. Moreau, D. Guyomard, J. Gaubicher, and F. Boucher, *Chem. Mater*., 2010, **22**, 4126.
9 K. Trad, D. Carlier, L. Croguennec, A. Wattiaux, M. Ben Amara, and C. Delmas, *Inorg. Chem.*, 2010, **49**, 10378.
10 W. Huang, B. Li, M. F. Saleem, X. Wu, J. Li, J. Lin, D. Xia, W. Chu, and Z. Wu, *Chem. Eur. J.*, 2014, **20**, 1
11 K. Trad, D. Carlier, A. Wattiaux, M. Ben Amara, and C. Delmas, *J. Electrochem. Soc*., 2010, **157**, A947.
12 P. Barpanda, T. Ye, S. Nishimura, S. C. Chung, Y. Yamada, M. Okubo, H. S. Zhou and A. Yamada, *Electrochem.Commun*., 2012, **24**, 116.
13 H. Kim, I. Park, D. H. Seo, S. Lee, S. W. Kim, W. J. Kwon,Y. U. Park, C. S. Kim, S. Jeon, and K. Kang, *J. Am. Chem. Soc*., 2012, **134**, 10369.
14 W. Huang, J. Zhou, B. Li, J. Ma, S. Tao, D. Xia, W. Chu, and Z. Wu, *Sci. Rep.,* 2014, **4**, 4188.
15 W. Song, X. Ji, Z. Wu, Y. Zhu, Y. Yao, K. Huangfu, Q. Chen and C. E. Banks, *J. Mater. Chem., A*, 2014, **2**, 2571.
16 R. Essehli, I. Belharouak, H. Ben Yahia, R. Chamoun, B. Orayech, B. El Bali, K. Bouziane, X. Zhou and Z. Zhen., *Dalton Trans*., 2015, **DOI:** 10.1039/C5DT00021A.
17 C. Delmas, M. Maccario, L. Croguennec, F. Le Cras, and F. Weill, *Nat. Mater*., 2008, **7**, 665.
18 S. Franger, F. Le Cras, C. Bourbon, and H. Rouault, *Electrochem. Solid-State Lett*., 2002, **5**, 231.
19 V. Petricek, M. Dusek, and L. Palatinus, *Z. Kristallogr*., 2014, **229**, 345.
20 V. Rodriguez-Carvajal, *Phys. B*., 1993, **192**, 55.
21 O. V. Yakubovich, M. A. Simonov, Yu. K. Egorov-Tismenko, and N. V. Belov, *Dokl. Akad. Nauk, SSSR*., 1977*,* **22**, 550.
22 I. D. Brown and D. Altermatt, *Acta Crystallogr*., 1985, **B41**, 244.
23 N. E. Brese and M. O'Keefe, *Acta Crystallogr*., 1991, **B47**, 192.
24 R. D. Shannon, *Acta Crystallogr*., 1976, **A32**, 751.
25 I. Belharouak and K. Amine, *Electrochem. Commun.*, 2005, **7**, 648.
26 R. Essehli, B. El Bali, A. Faik, S. Benmokhtar, B. Manoun, Y. Zhang, X.J. Zhang, Z. Zhou and H. Fuess, *J. Alloys Compd.*, 2012, **530**,178.
27 R. Essehli, B. El Bali, A. Faik, M. Naji, S. Benmokhtar, Y.R. Zhong, L.W. Su, Z. Zhou, J. Kim, K. Kang and M. Dusek, *J. Alloys Compd.*, 2014, **585**, 434.
28 K. Lasri, I. Saadoune, Y. Bentaleb, D. Mikhailova, H. Ehrenberg, L. Haggstrom and K. Edstrom, *Solid State Ionics*., 2012, **224**, 15.
29 T.G. Kima, J.G. Lee, D. Son, S. Jin, M. G. Kim, B. Park, *Electrochimica Acta.,* 2007, **53**, 1843–1849
30 N. Kalaiselvi, C.H. Doh, C.W. Park, S.I. Moon, M.S. Yun, *Electrochem. Commun*., 2004, **6**, 1110–1113